Chemical Engineering Journal 145 (2008) 316–327

Contents lists available at ScienceDirect

Chemical Engineering Journal

journal homepage: www.elsevier.com/locate/cej

Capturing sunlight into a photobioreactor: Ray tracing simulations of the propagation of light from capture to distribution into the reactor

Jan-Willem F. Zijffers*, Sina Salim, Marcel Janssen, Johannes Tramper, René H. Wijffels

Bioprocess Engineering Group, Wageningen University, P.O. Box 8129, 6700 EV Wageningen, The Netherlands

ARTICLE INFO

Article history:
Received 2 June 2008
Received in revised form 14 August 2008
Accepted 16 August 2008

Keywords:
Photobioreactor
Ray tracing
Light guide
Fresnel lens
Sunlight
Microalgae

ABSTRACT

The Green Solar Collector (GSC), a photobioreactor designed for area efficient outdoor cultivation of microalgae uses Fresnel lenses and light guides to focus, transport and distribute direct light into the algae suspension. Calculating the path of rays of light, so-called ray tracing, is used to determine local light intensities inside the photobioreactor based on the focused rays of sunlight. Reflection and refraction of the propagating rays of sunlight from point of focus to refraction into the photobioreactor is calculated. Refraction out of smooth and sandblasted distributor surfaces is simulated. For the sandblasted surface a specific structure is assumed and corresponding reflection and refraction patterns are described by a 2-dimensional modeling approach. Results of the simulations are validated by measurements on real light guide surfaces. The validated model is used to determine the influence of the solar angle on the uniformity and efficiency of light distribution over the light distributor surface.

The simulations show that efficient capturing of sunlight and redistribution inside the algal biomass can be achieved in the Green Solar Collector at higher elevation angles of the sun, making the Green Solar Collector suitable for operation at low latitudes with a high level of direct irradiance.

1. Introduction

The volumetric biomass productivity of a microalgae culture in a photobioreactor is determined by the light input in the photobioreactor and the efficiency of light use for microalgal growth. Light intensity is an important parameter for the photosynthetic efficiency in photobioreactors. Exposure to full sunlight intensities limits the microalgae's light use efficiency, while prolonged exposure to darkness stops the microalgae's autotrophic processes. To efficiently cultivate microalgae, the exposure to light has to be carefully regulated and therefore it is important to know local light intensities inside a photobioreactor [1,2].

The Green Solar Collector (GSC) [3] was developed to obtain high area biomass yields by efficiently capturing, transporting and redistributing available direct sunlight into the microalgae culture. It was designed to supply captured sunlight to the microalgae at reduced intensities. This in combination with a short light path and turbulent mixing is expected to result in high light use efficiency and high volumetric biomass productivity. To be able to run a light efficient cultivation an investigation into distribution of captured sunlight into the reactor compartment is necessary. A uniform distribution on the light distributor surface is needed to have a reduced and uniform light intensity inside the microalgae culture such that light can be efficiently used by the microalgae.

Extracting light uniformly from the lateral surfaces of optical fibers and light guide or distributor like structures has been a problem in previous research [4–6]. The problem was either caused by getting the light into the illumination plate [4] or getting the light out of the distributor over its lateral surface [5,6]. Csögör et al. [7] managed to improve the lateral distribution to a large extend by roughening the surface of the illuminating surface of the distributor. The short distance between the light source and the end of the distributor helped to achieve a more uniform illumination in the work performed by Csögör et al. [7].

Sunlight is captured into the GSC through polymethylmethacrylate (PMMA) Fresnel lenses that are able to rotate over two axes to follow the sun. The lenses can rotate over the light guide and the distance between the lens and light guide is adjustable to maintain the line of focus on top of the light guide as explained by Zijffers et al. [3]. Light focused on top of the light guides refracts into the light guides and internal reflection in the guides directs light into the bioreactor compartment. Internal reflection inside the guides and refraction out of the guides into the algal suspension is calculated based on the specific incident angles of sunlight rays on the interior surface of the light guide. Based on the relation between the light capturing surface of the lens and the light emitting surface of the light guide, the light intensity on the light distributor surface

* Corresponding author. Tel.: +31 317 483770; fax: +31 317 482237.
E-mail address: jan-willem.zijffers@wur.nl (J.W.F. Zijffers).

1385-8947/$ – see front matter © 2008 Elsevier B.V. All rights reserved.
doi:10.1016/j.cej.2008.08.011

will be about half of the sunlight intensity [3]. However, due to the changing position of the sun on the horizon and the position of the lens with respect to the sun, reflection and refraction of light on the lens and light guide vary. The results of a ray tracing study into the effect of changing reflection and refraction of light on the capturing efficiency and on the uniformity of light distribution will be discussed in this paper.

Ray tracing, "following a path of a photon (or ray of light) as it bounces around the scene" [8], can be used to determine the path of light rays and the intensity at which sunlight enters the microalgae culture. The path of the focused sunlight inside a light guide of the GSC is visualized for a guide with a smooth or a rough, sandblasted distributor surface. A specific surface structure for the sandblasted light guide surface is assumed, leading to specific reflection and refraction patterns for focused rays of sunlight.

The ray tracing routine is explained in a separate model description. The model is validated by comparing results of simulations with measurements of the refraction of focused light out of real light guides. Refraction and reflection of light is then simulated for different situations and the efficiency of light capturing and the uniformity of light distribution into the Green Solar Collector is discussed.

2. Model description

2.1. Ray tracing

The ray tracing approach used in this research regards sunlight as a bundle of parallel rays. All reflections and refractions of light on the internal and external surfaces of the lens and light guide are calculated by Snell's law and Fresnel's formula. Average values are used for the refractive indices of the different materials involved in the ray-tracing simulations, because only a minor change in refractive index occurs within the wavelength range studied (400–700 nm). These are: PMMA (lens and light guide): 1.49; water (algal suspension): 1.33; air: 1.00.

The calculation of the path of sunlight into the Green Solar Collector is split up in three parts, which are illustrated in Fig. 1:

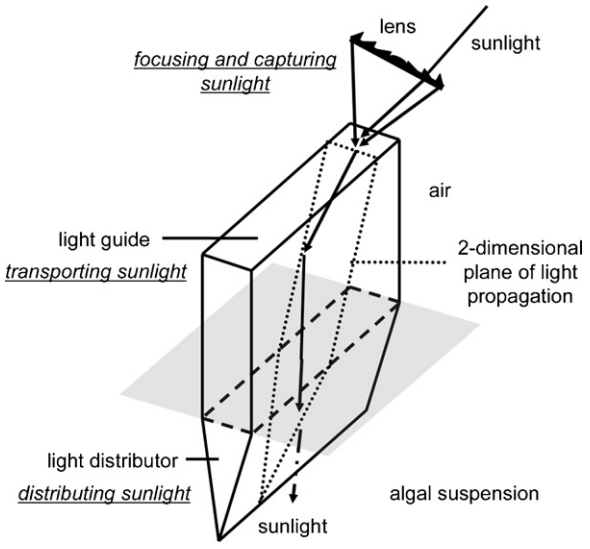

Fig. 1. Focusing and capturing, transporting, and distributing sunlight into the algal suspension. The lens has a width of 52 mm and a focal point at 51 mm. The total height of the light guide is 110 m, which can be split up in a rectangular part of 70 mm and a triangular part of 40 mm. Width of the light guide was chosen to be 8 or 16 mm.

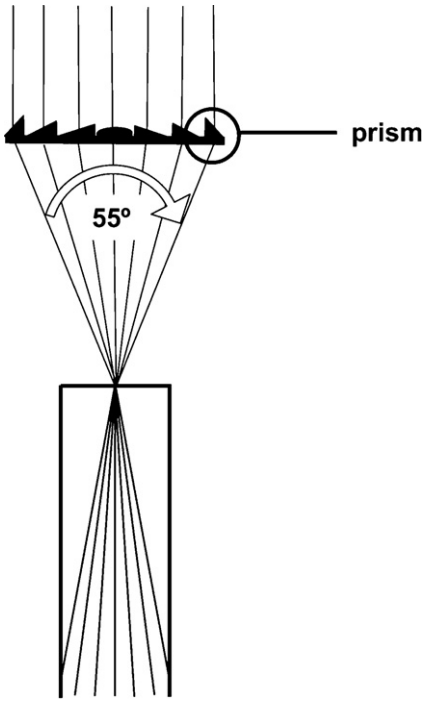

Fig. 2. Focusing of light by a Fresnel lens and capturing into the light guide.

1. Focusing of direct sunlight through a lens and capturing of focused light into the light guide.
2. Transport of captured light downwards through the rectangular top part of the light guide.
3. Re-distribution (refraction) of captured light out of the triangular bottom part of the light guide, i.e. the light distributor, into the algal suspension surrounding the triangular light distributor.

2.2. Focusing and capturing of sunlight

Sunlight is focused on top of the light guide by refraction of sunlight through the prisms of the Fresnel lens. The lens is positioned perpendicular to the sun such that sunlight is focused in a line on top of the light guide [3]. The width of this line is approximately 2 mm when focused perpendicularly on the light guide, at lower elevation angles of the sun the line widens to about 6 mm. Sunlight always strikes the lens perpendicular with respect to the width of the lens but not necessarily perpendicular with respect to the length of the lens.

The specific lens used on the GSC focuses sunlight in a window of 55° (Fig. 2). Since the ray tracing simulation requires a finite number of rays, each degree within the window of focus is considered to be a separate ray. A resolution per degree is chosen such that sufficient detail on the propagation of sunlight is obtained while maintaining reasonable computation times on a desktop computer. If desired, the model can be modified to use different windows of focus if other lens geometries are used on the GSC.

The intensity of each ray is calculated by correcting the radiant flux (Φ) of the direct sunlight for the incident angle (φ) of the sunlight with respect to the length of the lens and dividing it equally over 55 rays

$$\phi_{\text{ray}} = \frac{\phi_{\text{direct normal}} \times \cos(\varphi)}{55} \quad \text{(W)} \tag{1}$$

In passing the lens light is reflected twice. Once on the air–PMMA interface entering the lens and once on the PMMA–air interface leaving the lens. The amount of reflection on the interfaces

is calculated using the incident sunlight angle on the lens surface (φ). The amount of reflection on top of the light guide depends on the position of the lens with respect to the sun.

The sunlight rays are focused in a line on top of the light guide. The ray tracing results for a single 2-dimensional plane of light propagation, as shown in Fig. 1, can thus be extrapolated for the entire length of the lens. However, the length of the light guide has to be much larger than the height to be allowed to neglect the different geometry at beginning and end of the light guide.

2.3. Transporting captured light

All captured light propagates by total internal reflection inside the rectangular top part of the guide as long as it is surrounded by air and the surface of the guide is perfectly smooth [3]. The path of the refracted rays inside the light guide depends on the dimensions of the guide. All internal reflections on the light guide surface are perfect, i.e. no decrease in light intensity, and attenuation due to propagation in PMMA is assumed to be negligible. In fact, the light energy content of the ray will decrease somewhat, but it will be less than 1% while propagating inside the short, transparent PMMA light guide before reaching the triangular light distributor surface. This number is based on the average attenuation of PMMA for visible light.

2.4. Re-distributing captured light

Captured light must refract out of the light distributor surrounded by the algal suspension. Narrowing of the distributor towards the bottom causes rays to strike the distributor surface more perpendicularly and results in increased refraction of light out of the guide [9]. The distributor can have a smooth surface, but since internal reflection is no longer desired the surface can also be roughened to further facilitate refraction of light out of the guide.

2.4.1. Refraction of light out of a smooth distributor

Snell's law and Fresnel's formula are used to calculate the fraction of the radiant flux that reflects on the smooth distributor surface surrounded by the algal suspension. The reflected radiant flux of a ray (Eq. (2a)) is traced until all light is refracted out of the guide. Obviously, light that does not reflect on the surface will be refracted out of the guide (Eq. (2b)) and penetrates into the algal culture. The location where light refracts out of the distributor is calculated and determined for all 55 rays. A distribution profile of refracted radiant flux over the distributor surface can thus be created depending on the specific position of the sun

$$\phi_{\text{reflected ray}} = R \times \phi_{\text{ray}} \quad \text{(W)} \tag{2a}$$

$$\phi_{\text{refracted ray}} = (1 - R) \times \phi_{\text{ray}} \quad \text{(W)} \tag{2b}$$

2.4.2. Refraction of light out of a sandblasted distributor

To trace the rays during reflection or refraction on a rough surface, the structure of the surface needs to be known. According to Csögör et al. [7] an ideal rough surface can be considered to be a sphere emitter. The sandblasted distributor surface in the GSC is therefore assumed to be uniformly covered with infinitely small hemispherical dents. These hemispheres do not have any area; they are merely a tool to model the probable incident angles of a light ray on a sandblasted surface. The incident angles on the projection of the hemisphere on the 2-dimensional plane of light propagation (see Fig. 1) are determined based on the incident angle of the ray on the distributor surface.

Fig. 3 shows this 2-dimensional projection of a hemisphere with some possible incident angles. There is a certain part of the hemisphere where the sunlight cannot strike, i.e. the shadow side of the hemisphere, represented by E. The direction in which light can possibly reflect can be split up in two parts; the first one being reflections away from the surface, reflections B and C, the second being reflections towards the surface, reflections A and D. It is unclear which surface structure the light encounters that is reflected towards the surface on which the hemisphere is located, because, as explained before, the hemispheres are a tool to simulate the reflection on the sandblasted surface and have no actual area. In this study light that is reflected towards the surface is assumed to refract out of the sandblasted distributor surface.

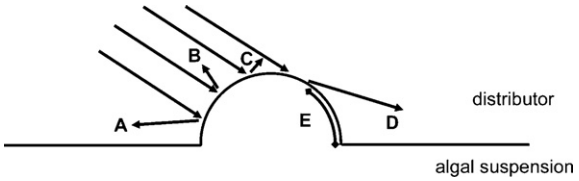

Fig. 3. Incident angles on a hemisphere.

To calculate the path of a ray after reflection, the angle of incidence on the sandblasted surface needs to be known. Fig. 4 shows an enlarged hemisphere on the light distributor and an enlarged ray represented by arrows R. The incident angle on the distributor surface is represented by angle δ. The number of possible incident angles on the imaginary hemisphere is thus angle δ plus 90°.

Each ray strikes a large part of the surface of the hemisphere and therefore the energy content of the ray has to be divided over several different incident angles on the 2-dimensional hemisphere. Again, a finite number of reflection and refraction events are required for the ray tracing simulation. Therefore these events are traced per whole degree on the hemisphere. The energy associated

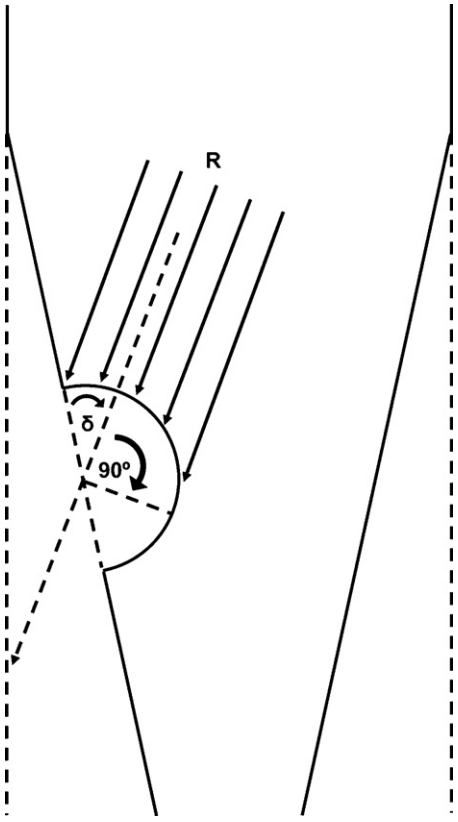

Fig. 4. Incident angles on an enlarged hemisphere on the sandblasted surface of the distributor.

with a certain angle and the corresponding reflection–refraction event depends on the cosine of that specific incident angle on the hemisphere with regard to the sum of the cosines of all possible incident angles on the hemisphere

$$\phi_{\text{angle}} = \cos(\text{angle}) \times \frac{\phi_{\text{ray}}}{\cos(-\delta)+\cos(-\delta+1^\circ)+\cdots+\cos(90^\circ-1^\circ)+\cos(90^\circ)} \quad (\text{W})$$

$$\phi_{\text{angle}} = \cos(\text{angle})\frac{\phi_{\text{ray}}}{\sum_{-\delta}^{90}\cos(\text{angle})} \quad (\text{W}) \qquad (3)$$

$$\text{Hence}: \quad \sum_{-\delta}^{90}\phi_{\text{angle}} = \phi_{\text{ray}} \quad (\text{W})$$

After each reflection–refraction event the amount of refracted light is determined and used to calculate the light intensity on the distributor at that position. The reflected remaining radiant flux is considered to be a new ray and is traced to the next encounter with an imaginary hemisphere on the opposite surface of the distributor. Based on the location of the initial incident ray and the direction of reflected rays, the locations where the reflected rays strike the opposite surface are precisely calculated. As a result, the light intensity distribution over the distributor surface can be determined using the amount of refracted light energy at all locations on the light distributor.

The reflections away from the surface can be split up in two parts. Light can reflect downwards or upwards into the distributor. A part of the upwards reflection will not come in contact with the sandblasted surface on the opposite side of the distributor, because it reflects upwards out of the distributor. These rays will reflect internally within the light guide and will be lost and are therefore not traced any further.

3. Materials and methods

3.1. Model validation

Perpendicular propagation of light focused by the lens and captured in the light guide was simulated using the Matlab software program and compared with the measured refraction of light out of real guides. Light was simulated to refract into an 8 mm wide light guide with a rectangular top part of 70 mm height and a light distributor part of 40 mm height surrounded by air. The simulated results are compared to the light intensity measured on the distributor surface. A smooth as well as a sandblasted distributor surface was simulated.

3.2. Light measurements at the distributor surface

Light was focused on top of the light guide by a halogen lamp and ellipse shaped reflector (Fig. 5). The validation was performed in air, because small underwater light sensors were not available. Validation in air also validated the under water situation, because the simulation was adjusted for the refractive index of air or water. Light entered the light guide perpendicularly relative to the guide length so that it reflected within a vertical 2-dimensional plane within the guide.

Based on the fact that an ellipse has two points of focus, an ellipsoid reflector was designed to focus light into a window of 55°, as shown in Fig. 6. A halogen lamp is placed in one point of focus and the top of the light guide in the other. The reflector is shaped such that the distance between the two points of focus is equal to the focal distance of the lens. Direct light from the lamp to the light guide is blocked, to assure only light from the reflector enters the light guide. The simulation results are corrected for the angles of focus that are blocked by the lamp cover. The lamp and reflector assembly could rotate over the light guide to mimic the rotation of the lens.

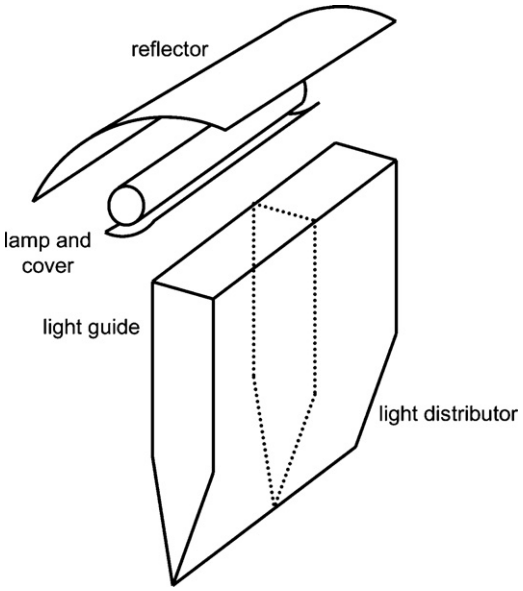

Fig. 5. Halogen lamp and reflector that can rotate over the light guide to resemble focusing of sunlight by the Fresnel lens, also see Fig. 9.

The light intensity was measured using three small 2 − π photodiode (∅ = 1.4 cm) facing the distributor surface in a dark room and covering the photodiode from residual stray light of the lamp. Fig. 7 shows the measuring positions on the distributor surface. Due to the size of the photodiode, measuring positions AL and AR (Fig. 7) cover a fraction of the light guide. However, no light refracts out of the rectangular light guide and all measured light at positions AL and AR is attributed to the surface fraction of the triangular distributor. The intensity was measured at 3 positions over the length of

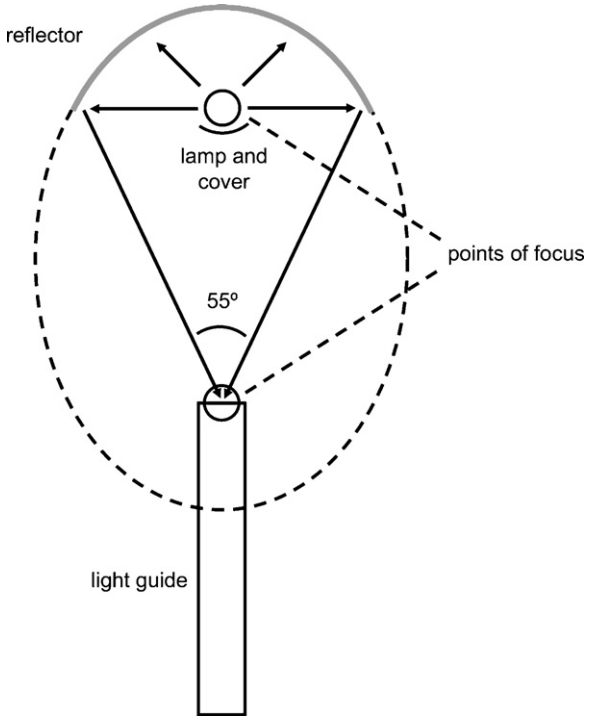

Fig. 6. An ellipsoid reflector, focusing light in a window of 55°.

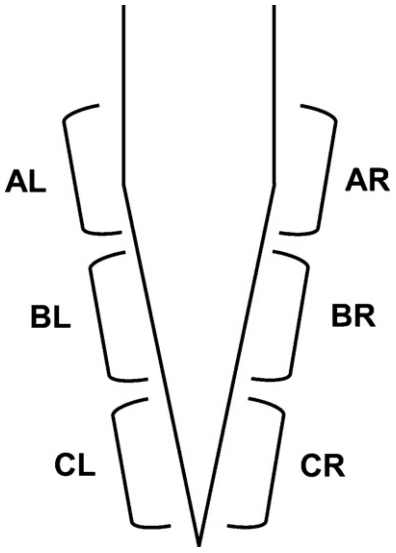

Fig. 7. Light measuring positions on the light distributor.

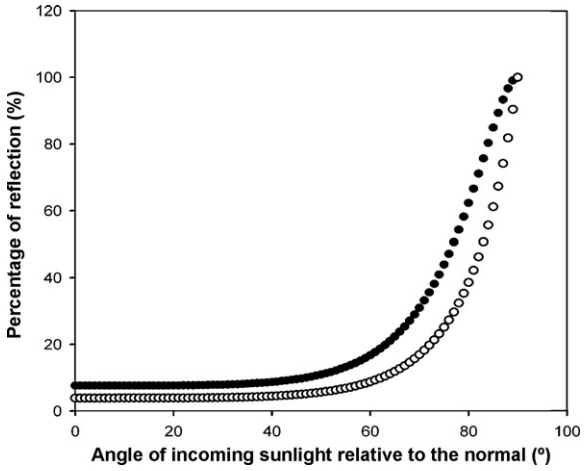

Fig. 8. Percentage of light that reflects in passing the lens (closed symbols) and in refracting through the top of the light guide (open symbols) at different incoming angles.

the distributor at 3 different heights on both the left and right side of the distributor (Fig. 7). It sums up to 18 measurements for one distributor to correct for deviations in the shapes of both light guide and distributor. In addition, five light guides—distributor combinations were used to validate the model to further reduce the effect of differences in shape in these hand made guides. The small photodiodes were calibrated against a LI-190SA quantum sensor (LI-COR Biosciences, Lincoln, USA). A smooth as well as a sandblasted distributor surface was measured and evaluated.

3.3. Simulation of the distribution of refracted light out of the distributor

Two light guides, one with a width of 8 mm and one with a width of 16 mm, but having the same height of 70 mm for the rectangular top part and 40 mm for the distributor, were simulated. The reflection and refraction pattern inside the guide and distributor were calculated and the light intensity at the distributor surface was determined. These simulations were done for distributors with a smooth and a sandblasted surface and assuming light enters the guide perpendicular with respect to the length of the light guide. However, during most of the day sunlight does not enter perpendicular to the length of the guide. The influence of the solar angle was simulated using the same model.

4. Results and discussion

4.1. Simulated amount of light loss in capturing of light into the light guide

In focusing of light by the Fresnel lens, a fraction of light will reflect away on the lens surface and is lost. To calculate the total amount of reflection on the lens, the incident angle of sunlight on the lens (φ) and the specific angle on the prisms, as shown in Fig. 2, have to be combined. The influence of the prisms on the amount of reflection is small. The maximum amount of reflection of light perpendicular to the length and width of the lens surface was 8% in passing the prism, compared to 7.6% on the flat surface in the middle of the lens. Therefore the lens was assumed to be flat and only the angle of the rays on the lens in the length direction was taken into account in calculating the percentage of reflection in passing the lens. The amount of reflection of light passing the lens, based on φ, is shown in Fig. 8. The percentage of reflection has its minimum value of 7.6% over a broad range of incident angles. But, reflection increases steeply at increasing incident angles from the normal on the lens.

In refraction of focused light into the guide, the rays encounter one air to PMMA interface, resulting in additional reflection losses as shown in Fig. 8. Since only one interface is passed, a lower percentage of reflection is obtained.

4.2. Simulated reflection and refraction inside the light guide and distributor

The propagation of captured light is traced within the light guide and re-distribution out of the distributor is determined. Fig. 9 shows an example of a result of the ray-tracing simulation in a 16 mm wide light guide and distributor. In the simulation, light is focused by a lens at an angle of rotation of 60°. Light strikes the top of the guide perpendicularly with respect to the length of the light guide. The focused sunlight enters through the top of the light guide exactly in the middle. The angle of each specific ray inside the light guide is calculated using Eq. (3) and Snell's law. A fraction of the radiant flux reflects from the light guide (see Fig. 8), which is shown by the black mark on the point of entry. The 55 rays of sunlight, represented by the gray lines, propagate downward by internal reflection on the light guide–air interface. No light leaves the guide at this stage, hence the absence of the black marks on the outside of the rectangular part of the light guide. As soon as the light hits the surface of the triangular light distributor surrounded by the algal suspension, light leaves the light guide. Radiant flux refracts out of the distributor, shown by the black marks on the distributor surface. The gray lines propagate further downward until all radiant flux has refracted out of the distributor. The black marks are only shown when more than 1% of the radiant flux of the original ray refracts out of the distributor.

4.3. Model validation

The measured and simulated values for the light intensity distribution are compared in Figs. 10 and 11. Fig. 10 shows the measured and simulated results for the light intensity leaving the smooth light guide at the positions indicated in Fig. 7. The focused light enters at different rotation angles of the lens or lamp; a small angle corresponds to a more perpendicular entry of focused light into the

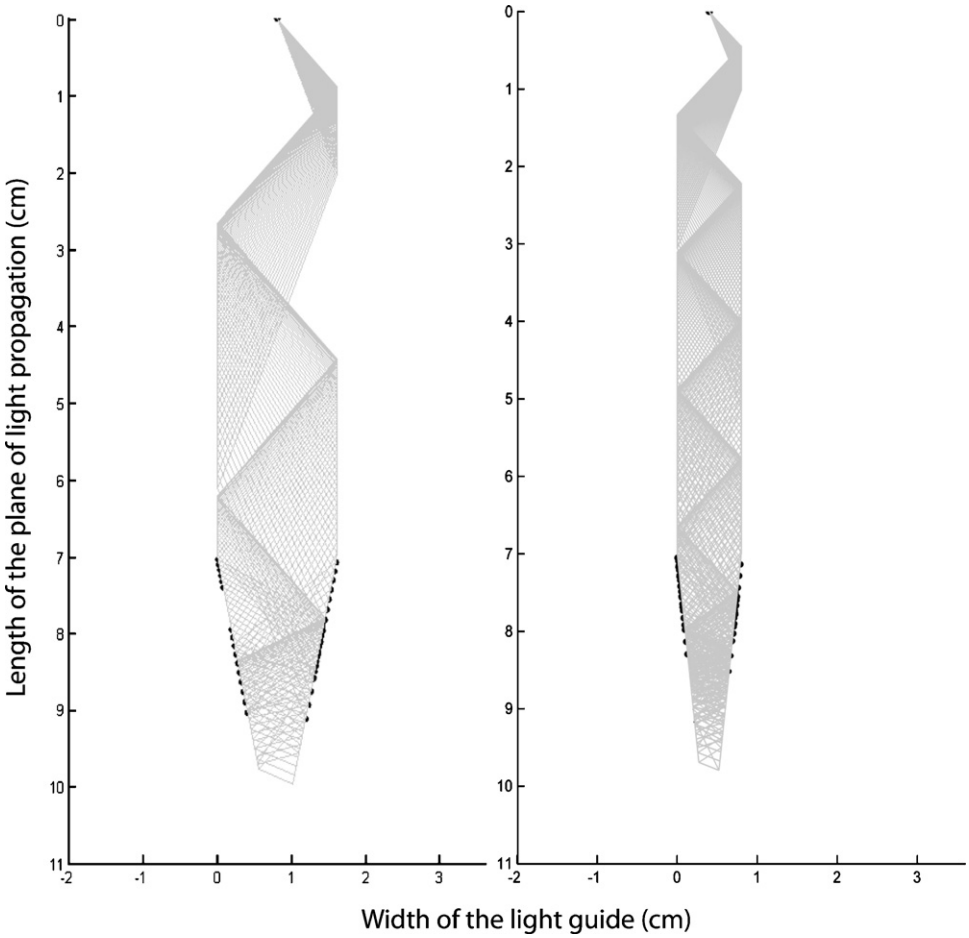

Fig. 9. Simulated reflection into and refraction out of a 16 mm and 8 mm wide light guide with a smooth distributor surface. Light strikes the guide perpendicularly with respect to the length of the light guide. The light is focused by the lens at an angle of rotation of 60°.

guide. The general pattern of the light intensity over the surface of the light guide fits the measured results well. However, deviations exist due to non-perfect focusing of light by the ellipse shaped reflector and reflection of light from the small metal plate shielding the light guide from light directly from the lamp (Fig. 5). Instead of the modeled perfect line of focus, the reflector produces a wider line of focus covering a large part of the upper surface of the light guide. A 12 mm diameter linear tungsten halogen lamp was used that showed a bright light radiating wire throughout the measurements. The diameter of this wire was approximately 1 mm. In case of perfect focus of this light, the line of focus on the light guide would also be approximately 1 mm.

This wide line is the cause that a fraction of the light is not focused on top of the light guide at large incoming angles. This explains the deviation between modeled and measured light intensities at the rotation angles of 60° and 75° where the modeled results are consistently higher than the measured light intensity (BR and BL in Fig. 10). The line on top of the guide of sunlight focused by the lens on the actual GSC also has a width of 2–6 mm and will therefore show results in-between the results of the lamp and model. Stray light causes the measured results to deviate from the modeled results in case the light intensity calculated by the model is zero. Taking into account the fact that the model simulates a perfect situation, it gives a good approximation of local light intensities leaving the light guide.

The simulated results for the sandblasted light guide surface (Fig. 11) show a similar trend to the measured results, taking into account the non-perfect focusing by the ellipse reflector. The differences in the results, especially for positions CL and CR can be attributed to the underestimation of the reflection downwards due to the 2-dimensional representation of a 3-dimensional hemispherical dent, as explained in Appendix A.

The result of the 2-dimensional simulation underestimates the amount of light that reflects downward inside the distributor, especially at incident angles more perpendicular to the width of the light guide. The underestimation will be more apparent when the light guide is surrounded by air as can be seen in the results of the validation experiments (Fig. 11). Apart from this weakness, the measured results for the smooth as well as the sandblasted distributor surface surrounded by air (Figs. 10 and 11) show the same trend as the modeled results. Therefore local light intensities on the distributor surface surrounded by the algal suspension can be estimated by the relatively simple 2-dimensional approach.

4.4. Simulated distribution of light refracted out of the guide submerged in the algal suspension: the effect of guide dimensions and surface structure

The validated model is used to do a more detailed investigation into the influence of changes in the dimensions of the guide and the influence of sandblasting the distributor surface on the light distribution out of the distributor.

If the surface of the distributor is smooth, most of the light will either completely refract out of the guide or completely reflect

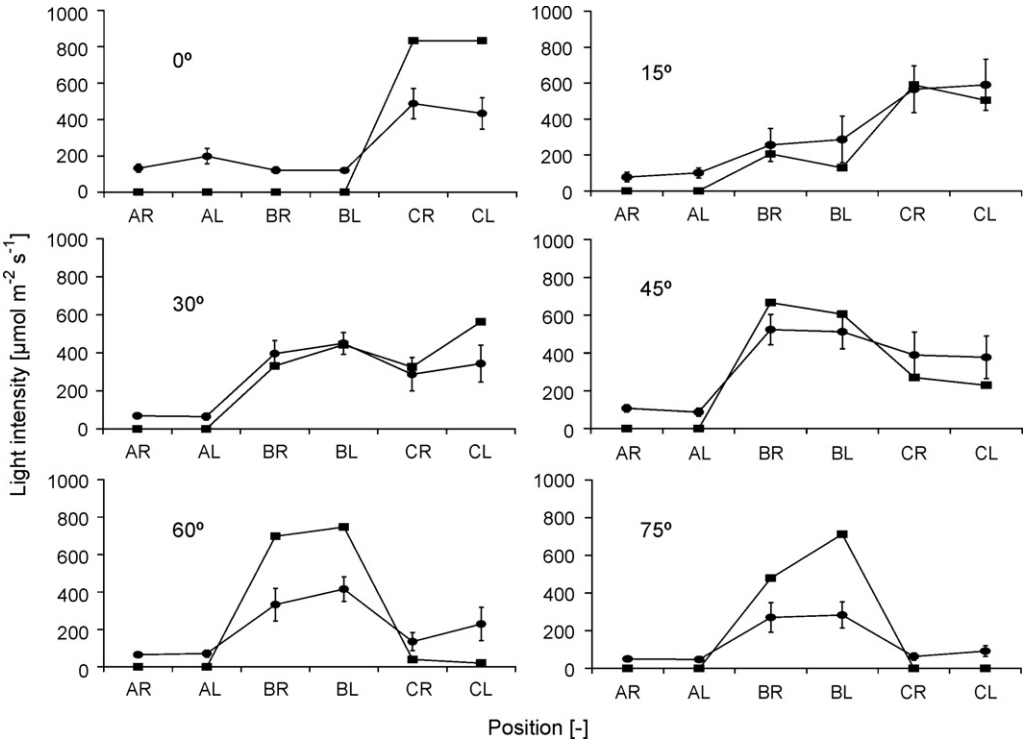

Fig. 10. Light intensity leaving the smooth light guide at different rotation angles of the lens (simulated; square symbols) or rotation of the lamp (measured; round symbols).

further into the guide on the first encounter of the rays with the interface of the distributor and algal suspension. At angles of 63° or larger from the normal on the smooth distributor–suspension interface the total ray will reflect on the interface. At smaller angles light will almost completely refract out of the guide. At an angle of 53° for example, 97.5% of the light energy will refract out of the guide and only the remainder reflects internally. Gradual leakage of light from the guide into the algal suspension during the day is thus not possible due to the varying position of the sun in the sky.

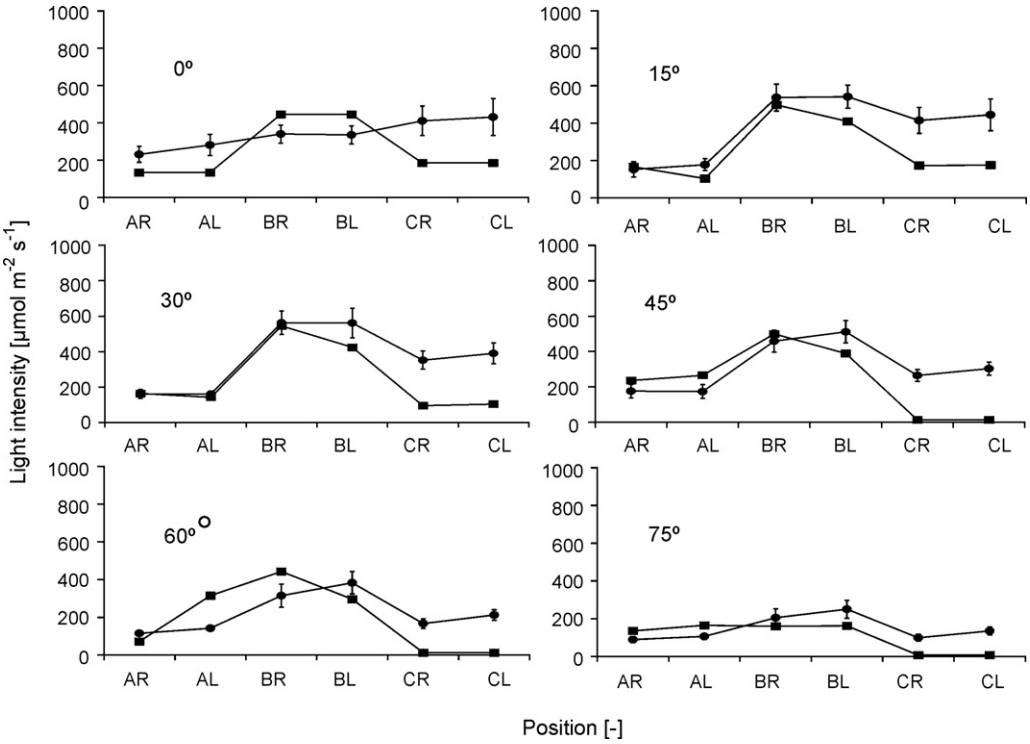

Fig. 11. Light intensity leaving the sandblasted light guide at different rotation angles of the lens (simulated; square symbols) or rotation of the lamp (measured; round symbols).

Total internal reflection does not occur on the sandblasted surface, because the original ray on the distributor surface strikes the hemisphere at a multitude of angles, causing a large fraction of the radiant flux to refract into the algal suspension.

The dimensions of the light distributor part of the light guide are of influence on the amount of light leaving the guide and on the uniformity of light distribution. The reflection and refraction pattern in the light guide changes with the ratio of width to height of the distributor, because the angles of incidence of the rays on the distributor surface change.

A wider light guide causes a decrease in the incident angle of the incoming ray relative to the normal of the interface, causing light to refract out of the guide. It also causes the triangular bundle of focused rays to be more spread out over the distributor surface in the wider light guide, especially at larger angles of rotation of the lens. This can be seen by comparing the propagation in the guides shown in Fig. 9. This is also shown in Appendix B, which shows the radiant flux distribution on the distributor surface for two distributors with different width and surface structure. Since light is more spread out over the surface of the wide distributor it causes a somewhat more uniform distribution of the radiant flux over its surface at rotation angles of the lens of 30° and larger. In a narrow distributor, at rotation angles of 15° and 30°, a large fraction of the rays will strike the smooth distributor–suspension interface at an angle larger than 63° from the normal and will therefore cause internal reflection. A larger fraction of the radiant flux will reflect internally and will therefore lead to a more uniform distribution over the distributor surface. However, at a rotation angle of 0° too much internal reflection occurs on the smooth surface causing again a decrease in uniformity of light distribution.

Sandblasting the surface does not result in a more uniform distribution of refracted light at larger rotation angles of the lens. In this case most of the rays will have a small angle of incidence relative to the normal on the hemispheres on the sandblasted surface, causing light to refract out of the guide.

At rotation angles of the lens of 15° and 30° on the narrow light guide, sandblasting causes less uniform distribution, because the amount of internal reflection is diminished due to the hemispheres on the distributor surface. Reflection on the hemispheres causes less light to propagate downwards compared to internal reflection in the smooth distributor. However, the results shown in Appendix B underestimate the reflection downwards into the sandblasted distributor as explained in Appendix A. But, no drastic improvement in the distribution can be expected, since the majority of the light will refract out of the distributor upon the first encounter with the hemisphere.

In the wider light guide the sandblasting of the distributor also causes less internal reflection at rotation angles of 15° and 30° and thus more reflection out of the top of the distributor. But, because the triangular bundle of focused rays is more spread out over the distributor surface, the distribution is more uniform compared to the narrower light guide.

The distribution at a rotation angle of 30° is better on the smooth distributor surfaces, compared to the sandblasted surfaces and also the light intensity on the complete distributor surface is less than the solar intensity. However in all other situations, a wider sandblasted distributor is preferred.

4.5. Simulated reflection and refraction pattern based on the position of the sun

The previous discussion was based on results of simulations where light entered the guide perpendicular to the length of the guide with the lens rotating over the light guide. When the position of the sun is taken into account, the dimensions of the 2-dimensional plane of light propagation (illustrated in Fig. 1) will change as can be deduced from Fig. 12 when compared to Fig. 9. The same simulation procedure is used to calculate the reflection and refraction pattern in the guide, taking into account its new dimensions. Fig. 12 shows the pattern for light focused by the Fresnel lens that strikes the top of a smooth light guide at a rotation angle of 60° relative to the width and a 60° angle relative to the length. The plane in which the rays are traced is similar to the situation in Fig. 9. Using Snell's law, the angle of refraction of the plane is calculated to be 35.5° relative to the length of the light guide (also see Fig. 1). Therefore the plane increased in length by a factor of $\cos^{-1}$ (35.5°).

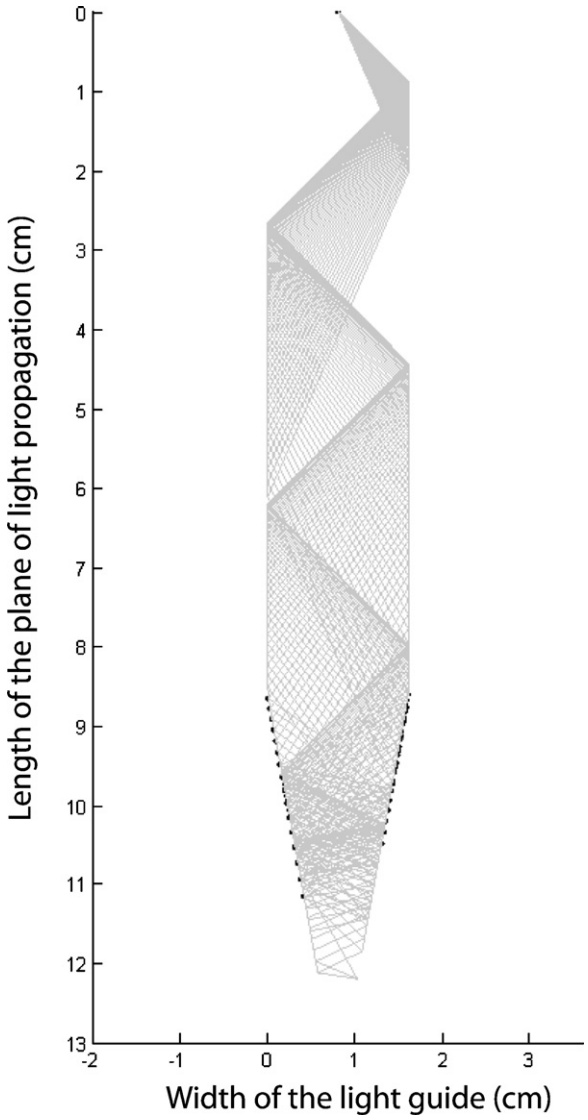

Fig. 12. Simulated reflection in and refraction out of a 16 mm wide light guide with a smooth surface. Light strikes the guide at an angle of 60° with respect to the length of the light guide (also see Fig. 1) the light is focused by the lens at an angle of rotation of 60°.

The refraction pattern inside the light guide changes when the orientation of the plane of light propagation within the light guide changes. This has no effect on the angle of incidence on the surface in the rectangular top part of the guide, where light still propagates through internal reflection. However, when the light distribution on the distributor surface for the 16 mm wide light guides in Figs. 9 and 12 are compared, the gap on the upper left surface of the distributor in Fig. 9 where light does not refract out

of the guide is gone in Fig. 12. If light does not enter perpendicularly, the plane in which light rays are traced increases in length. The increase causes light to reflect at a different location in the guide changing the reflection and refraction pattern. The increase in length also has an influence on the imaginary dimensions of the distributor part in the 2-dimensional plane of light propagation. This part also becomes longer, creating a relatively narrower distributor and consequently changing the reflection and refraction pattern. A narrower distributor leads to a less uniform distribution of light over its surface when light enters less perpendicular with respect to the width of the guide. To have the best light capturing efficiency and most uniform distribution of light, a more perpendicular entry of light is desired.

Predicting the distribution of light out of the distributor at forehand based on the dimensions of the light guide and distributor is difficult because dimensions of the plane of light propagation change with changing position of the sun. It results in a continuously changing reflection pattern not only in the distributor, but also in the rectangular top part. Therefore, optimal dimensions of guide and distributor cannot be predicted based on the results of a few situations. Extensive ray tracing of sunlight is needed to know the light distribution on the distributor surface throughout the day. Based on the results for all angles of elevation and azimuth of the sun a balanced choice for the dimensions of the light guide and distributor can be made to have the best distribution on light on the distributor surface.

5. Conclusions

Local light intensities at the surface of the distributor in the Green Solar Collector can be calculated trough ray-tracing of focused direct sunlight. Results of simulations of refraction of light out of the distributor surface show the same trend as the measured results. The light capturing efficiency into the light guide is high and almost all captured light can be distributed into the algal suspension. However, from the results it also becomes clear that a uniform distribution of light over the entire surface of the distributor cannot be achieved during the entire day due to the large variation in incident angles of sunlight. At light entering at small angles from the normal, the uniformity of light distribution is much better. Scattering of light by the microalgae will further distribute the light throughout the algal suspension, especially at low biomass concentrations. The GSC, however, is designed for cultivating the algae at high biomass concentrations and in this situation light will be completely absorbed at several millimeters from the distributor surface. A uniform distribution is required to supply the correct light regime in this case.

A specific surface structure, other than the triangular shape and the sandblasted surface, might help to overcome the problems of non-uniform irradiation as mentioned by Gordon [10]. But, these tailor made structures will only work with constant incoming angles of light, such that light always strikes the distributor surface at the same position. However, the focused sunlight strikes the distributor surface at varying positions during the day and the tailored structures can therefore not be used in the Green Solar Collector.

During the day however, the position of the sun in the sky changes, changing the incident angles on the lens and light guide. These angles determine the light capturing efficiency, which depends on location of the GSC, orientation with respect to the sun, and date and time. As can be seen in Fig. 8, the reflection on the lens and light guide is at its minimum at an angle of 40° and less. The same applies for the loss on the light guide, which is also lowest at rotation angles of 45° and smaller. If Fig. 8 and Appendix B are combined, it is clear that capturing of light at low elevation angles of the sun is poor. At elevation angles of 45°, the total capturing efficiency of direct sunlight into the light guides already is 80% and it increases up to 89% for a perpendicular focusing of sunlight. The GSC is therefore best suited for operation at locations at low latitudes, where the sun quickly rises to high elevation angles and the intensity of direct light is highest.

Our work clearly shows that the Green Solar Collector is most suited for operation at locations at low latitudes. At low latitudes, the sun rises and settles quickly and has a high elevation angle during most of the day. In this situation it is especially beneficial to reduce the (over-) saturating intensity of direct sunlight before illuminating the microalgae, since it results in an increased productivity compared to exposure to full sunlight as shown by Qiang et al. [11,12]. If the GSC is located such that the lens stretches from east to west the light distribution will be most uniform, because during the larger part of the day light enters at an angle of less than 30° from the normal. It results in an efficient capturing (Fig. 8) and an increased uniformity of sunlight distribution out of the 16 mm wide sandblasted light guide at intensities which are about equal or less then the intensity of sunlight.

Acknowledgement

This work was financially supported by the EU/Energy Network project Solar-H (FP6 contract 516510).

Appendix A

A.1. Reflection and refraction on a 3-dimensional hemispherical dent

The ray of sunlight can strike at a number of locations on the hemisphere as previously explained in Fig. 4. It was assumed that a ray of sunlight will always strike the hemisphere on the circular band formed by the projection of the hemisphere on the plane of light propagation (also see Fig. 1). But, the ray can also strike the hemisphere at other locations as illustrated by the dotted arches in Fig. 13.

The difference in incident angles on the hemisphere surface in this more realistic 3-dimensional situation compared to the 2-dimensional approach results in a change in reflection and refrac-

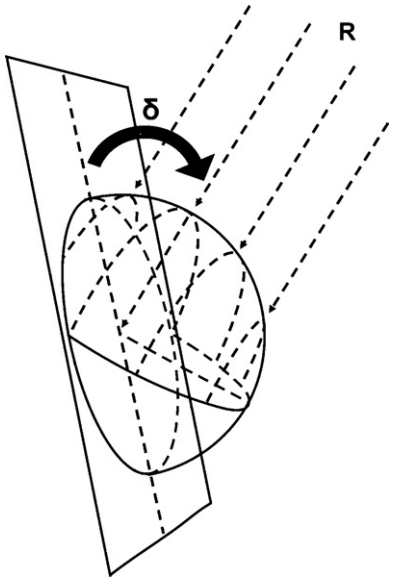

Fig. 13. 3-Dimensional representation of a hemispherical dent on the sandblasted distributor surface.

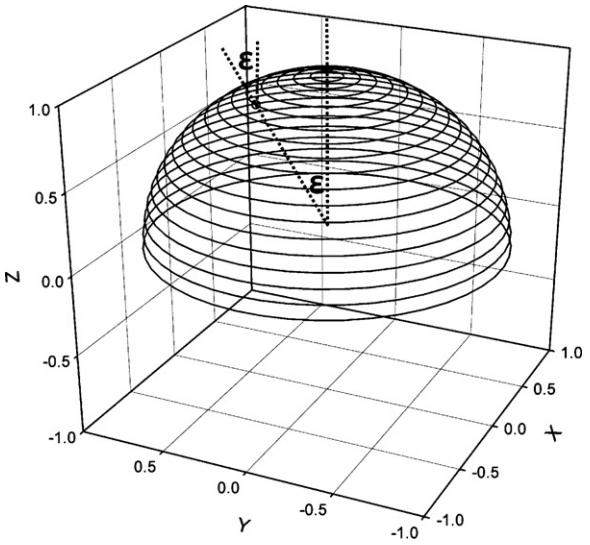

Fig. 14. Circular bands on a hemisphere corresponding to equal incident angles when struck by a vertical ray (bands at a 5° incident angle interval).

tion pattern. However, the difference is small enough to allow the use of the more simple 2-dimensional approach as explained below.

Fig. 14 shows circular bands that correspond with equal incident angles (ε) when a vertical ray strikes the surface of the hemisphere. The vertical ray can be seen as an incident ray of light perpendicular on the distributor surface ($\delta = 90^\circ$, Fig. 13). The amount of radiant flux associated with a certain incident angle on the hemisphere surface is calculated using Eq. (4). It depends on the cosine of ε and the length of the circular band around the hemisphere at that angle, which changes with the sine of ε (Fig. 14)

$$\phi_\varepsilon = \cos(\varepsilon)\,\sin(\varepsilon)\,\frac{\phi_{\text{ray}}}{\sum_0^{90}\cos(\varepsilon)\times\sin(\varepsilon)} \quad (\text{W})$$
$$\text{Hence}: \sum_0^{90}\phi_\varepsilon = \phi_{\text{ray}} \quad (\text{W}) \tag{4}$$

Fig. 15 shows the percentage of the radiant flux that reflects away from the hypothetical 2- or the real 3-dimensional hemisphere, considering a ray which strikes the complete hemisphere surface.

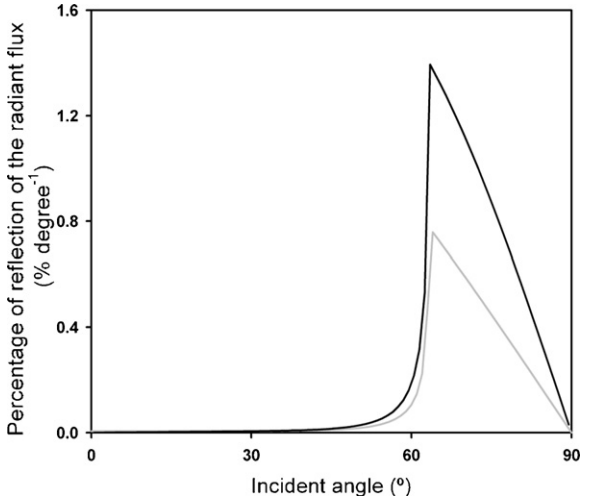

Fig. 15. Percentage of reflection on a surface of a 2-dimensional hemisphere (gray) and on a 3-dimensional hemisphere (black) depending on the angle from the normal ($90^\circ - \varepsilon$) on the surface.

The percentage of reflection is calculated for the situation when the hemisphere is on the distributor–algal suspension interface. The energy associated with each incident angle on the 2-dimensional hemisphere is calculated using Eq. (3) ($\delta = 0$). The energy associated with each incident angle on the 3-dimensional hemisphere is calculated using Eq. (4). The reflection at each incident angle is calculated using Snell's law and Fresnel's formula (Appendix A). The smaller incident angles that incorporate most of the light energy will almost completely refract out of the distributor as can be seen from Fig. 15. From an incident angle of around 55° on the hemisphere, reflection of light energy increases. Upon further increase in angle the amount of reflection decreases again due to the decrease in energy content associated with that angle.

If angle δ on the distributor surface (Fig. 13) is 90°, 12% of the radiant flux reflects in the 2-dimensional case and 22% in the 3-dimensional case. The 10% difference is due the fact that in the 3-dimensional case there is a larger hemisphere surface fraction where light strikes at a large angle. If sunlight enters the light guide more perpendicularly with respect to the width of the guide, angle δ will be smaller and the ray can only strike on a fraction of the hemisphere surface. This fraction covers less surface area where light strikes at a large angle, decreasing the total amount of reflection on the 2- as well as the 3-dimensional hemisphere surface (Fig. 15).

If angle δ is more perpendicular however, the 2-dimensional representation coincides most with the real 3-dimensional situation, because the direction of the reflected light needs to be taken into account. In the 3-dimensional situation the reflected light at δ approaching 90° is more directed towards the surface of the distributor, because radiant flux reflects at angles larger than 45° (Fig. 15) resulting in reflected light directed towards the distributor surface which refracts out of the distributor (also see Figs. 3 and 13). In this case, in both the 2- and 3-dimensional representations all radiant flux will refract out of the guide, either by refraction at small incident angles or reflection towards the distributor surface.

When angle δ becomes smaller, the difference between the 2-dimensional representation and the real 3-dimensional situation is larger. Although less light will reflect on the hemisphere surface compared to the perpendicular case, the reflected light on the hemisphere is not directed towards the distributor surface, but is directed downwards into the distributor. Consequently, in the real 3-dimensional situation more light will reflect downwards into the distributor as compared to the 2-dimensional representation. The worst-case scenario for difference between the 2-dimensional representation and the real 3-dimensional situation occurs when angle δ is 0°. In this situation the amount of reflection is the same as in case δ is 90°, but none of the reflected light is directed towards the distributor surface; it all reflects further downward into the distributor.

Reflection appears to be low anyhow since a minimum of 78% of the radiant flux will refract out of the distributor on the first encounter with the sandblasted surface in the 3-dimensional representation. In the 2-dimensional representation a minimum of 88% of the radiant flux refracts out of the distributor. Taking all the above into consideration, the more simple 2-dimensional approach provides a useful simulation of the real 3-dimensional sandblasted surface surrounded by the algal suspension.

Appendix B

The lens focuses sunlight with an intensity of 2500 μmol photons m^{-2} s^{-1}. Values shown in Table 1 represent the average light intensity in μmol photons m^{-2} s^{-1} over the different surface fractions of the distributor surface. It is divided into 5 equal fractions on the left and right surface. Fraction 1 is

Table 1 Simulated light distribution over the left and right vertical surface of the distributor in the algal suspension in two different light guides at various rotation angles of the lens

Angle of rotation of the lens	Fraction of the light distributor surface	Smooth surface				Sandblasted surface			
		8 mm wide		16 mm wide		8 mm wide		16 mm wide	
		Left	Right	Left	Right	Left	Right	Left	Right
0°	1	0	0	568	568	1841	1841	1595	1595
	2	472	472	125	125	1715	1715	1620	1620
	3	1701	1701	919	919	1776	1776	1245	1245
	4	2482	2482	3071	3071	1079	1079	1302	1302
	5	2299	2299	2123	2123	431	431	991	991
	Refracted into the algal suspension	88.00		88.80		88.24		88.28	
	Loss on top of the guide	3.60		3.60		3.60		3.60	
	Reflection backwards	–		–		0.56		0.52	
15°	1	127	1139	781	240	1852	2561	1827	1136
	2	580	1396	125	1466	1707	2177	1619	1827
	3	1397	1286	429	1851	1117	1523	1217	1497
	4	2075	1626	1693	3734	856	1027	1276	1319
	5	2011	2155	2123	1132	431	431	991	566
	Refracted into the algal suspension	88.72		88.72		88.17		88.22	
	Loss on top of the guide	3.68		3.68		3.68		3.68	
	Reflection backwards	–		–		0.55		0.50	
30°	1	1565	1854	781	1444	2818	3255	931	2310
	2	1550	1926	1573	1466	2419	2159	2349	2082
	3	1398	1322	1255	1626	855	860	1712	1427
	4	1587	896	1673	2171	347	574	850	1032
	5	910	711	527	1001	294	63	600	162
	Refracted into the algal suspension	88.24		88.24		87.75		87.84	
	Loss on top of the guide	4.16		4.16		4.16		4.16	
	Reflection backwards	–		–		0.49		0.40	
45°	1	3319	3031	3055	1444	4070	3955	3170	1414
	2	2023	1946	1808	2325	2379	1904	2556	2248
	3	1152	1322	1016	1492	390	363	1640	981
	4	242	342	105	1906	80	97	92	813
	5	0	0	29	0	35	41	108	114
	Refracted into the algal suspension	86.04		86.04		85.64		85.75	
	Loss on top of the guide	6.36		6.36		6.36		6.36	
	Reflection backwards	–		–		0.40		0.29	
60°	1	3916	4506	2274	1510	3954	4476	2243	1479
	2	1563	1644	1689	4453	1415	1612	1634	4390
	3	217	39	1020	721	99	71	953	708
	4	0	1	37	6	74	68	89	27
	5	0	0	0	0	38	31	77	78
	Refracted into the algal suspension	76.45		76.45		76.14		76.24	
	Loss on top of the guide	15.95		15.95		15.95		15.95	
	Reflection backwards	–		–		0.31		0.21	
75°	1	3550	3439	2274	137	3482	3368	2242	138
	2	508	720	1689	3021	458	664	1631	2982
	3	0	0	970	19	37	42	942	7
	4	0	0	0	0	44	45	6	27
	5	0	0	0	0	26	22	23	78
	Refracted into the algal suspension	52.85		52.85		52.65		52.73	
	Loss on top of the guide	39.55		39.55		39.55		39.55	
	Reflection backwards	–		–		0.20		0.12	
90°	1	2348	1548	1345	137	2304	1519	1327	137
	2	473	208	6	3012	453	190	1	2980
	3	0	0	9	0	5	15	3	2
	4	0	0	0	0	1633	65		
	5	0	0	0	0	11	17	23	15
	Refracted into the algal suspension	29.44		29.44		29.35		29.38	
	Loss on top of the guide	62.96		62.96		62.96		68.96	
	Reflection backwards	–		–		0.09		0.06	

the top of the distributor surface and Fraction 5 is the bottom of the distributor surface. The lens is positioned towards the left side of the light guide. Percentage of the total sunlight that refracts into the algal suspension is presented as well as percentage of light loss on top of the light guide and percentage of reflection backwards due to sandblasting of the distributor surface. Light enters perpendicularly on the lens; reflection in passing the lens is thus constant at 7.6% (Fig. 8). Reflection on top of the light guide causes light loss at all rotation angles. However at rotation angles of 63° and larger not all light can be focused on top op the light guide, resulting in an increased light loss on top of the guide.

Loss of light on top of the guide increases steeply at larger angles of rotation, similar to Fig. 8. However, since the light is focused in a window of 55°, loss of light at rotation angles of 90° is less than 100%, even though a fraction of the focused sunlight is not being focused on top of the guide.

References

[1] J. Pruvost, J. Legrand, P. Legentilhomme, A. Muller-Feuga, Aiche J. 48 (5) (2002) 1109–1120.
[2] I. Perner-Nochta, C.J. Posten, Biotechnology 131 (3) (2007) 276–285.
[3] J.W.F. Zijffers, M. Janssen, J. Tramper, R.H. Wijffels, Mar. Biotechnol. 10 (4) (2008) 404–415.
[4] J.Y. An, B.W. Kim, J. Biotechnol. 80 (1) (2000) 35–44.
[5] S. Hirata, M. Hayashitani, M. Taya, S. Tone, J. Ferment Bioeng. 81 (5) (1996) 470–472.
[6] O. Pulz, N. Gerbsch, R. Buchholz, J. Appl. Phycol. 7 (2) (1995) 145–149.
[7] Z. Csögör, M. Herrenbauer, I. Perner, K. Schmidt, C. Posten, Chem. Eng. Process 38 (4–6) (1999) 517–523.
[8] A.S. Glassner, An Introduction to Ray Tracing, Academic Press, London, 1989, p. 329.
[9] H. Ries, A. Segal, Karni, J. Appl. Optics 36 (13) (1997) 2869–2874.
[10] J.M. Gordon, Int. J. Hydrogen Energy 27 (11–12) (2002) 1175–1184.
[11] H. Qiang, Y. Zarmi, A. Richmond, Eur. J. Phycol. 33 (2) (1998) 165–171.
[12] H. Qiang, D. Faiman, A. Richmond, J. Ferment Bioeng. 85 (2) (1998) 230–236.